International Journal of Pharmacology

ISSN 1811-7775

science alert

ansinet
Asian Network for Scientific Information

OPEN ACCESS International Journal of Pharmacology

ISSN 1811-7775
DOI: 10.3923/ijp.2022.644.656

Research Article
Predictive Analysis of COVID-19 Symptoms with CXR Imaging and Optimize the X-Ray Imaging Using Segmentation Thresholding Algorithm-An Evolutionary Approach for Bio-Medical Diagnosis

[1]N. Prabhakaran, [2]S. Anandha Prasad, [2]M. Kamali, [3]C. Sabarinathan, [4]I. Chandra and [5]V. Prabhu

[1]Department of Biomedical Engineering, Agni College of Technology, Chennai, India
[2]Department of ECE, Vel Tech High Tech Dr. Rangarajan, Dr. Sakunthala Engineering College, Avadi, 600 062, Chennai, India
[3]Department of CSE, SRM University, Vadapalani Campus, India
[4]Department of ECE, Rajalakshmi Institute of Technology, Thandalam, Chennai, India
[5]Department of ECE, Vel Tech Multi Tech Dr. Rangarajan Dr. Sakunthala Engineering College, Avadi, 600 062, Chennai, India

Abstract

Background and Objective: The concept of Too Close and Too Short spreads the virus simultaneously from one person to another person. The radiologist investigates to prevent the spreading of the virus in the earlier stage of diagnosis and predict the symptoms in the beginning stage. The objective of the study is to predict the virus in the earlier stage and diagnose it so that the mortality rate is reduced. Hence, the virus-infected person lives a healthier life. **Materials and Methods:** The Chest X-ray imaging segments the image concerning edge detection (with and without contour detection) for earlier identification and prediction of COVID-19 symptoms. The segmentation thresholding algorithm accurately detects the parameters of fever, pneumonia and mucus fluid in earlier predictions. Moreover, the segmentation thresholding algorithm automatically classifies with the prediction of COVID-19 symptoms in pixel shape, size and intensity. Extraction of image features for pixel size, shape and intensity for feature enhancement and measurement. **Results:** Validation of segmentation thresholding algorithm improves with high accuracy in Chest X-ray imaging. The predictive analysis of CXR imaging to Accuracy, Precision, F-measure and Recall accurately enhanced with symptoms of COVID-19 in an earlier stage. The future study of the proposed method detection of COVID-19 symptoms is predicted in the earlier stage can be diagnosed automatically. **Conclusion:** Detection of COVID-19 symptoms in earlier stage processed through CXR imaging via Automatic Segmentation Threshold Algorithm clusters the pixel concerning contour and non-contour edge detection. The accuracy detection of contour and non-contour edge detection extract the image feature 90% of the original enhanced image.

Key words: COVID-19, too close too short, radiologist and chest X-ray

Citation: Prabhakaran, N., S.A. Prasad, M. Kamali, C. Sabarinathan, I. Chandra and V. Prabhu, 2022. Predictive analysis of COVID-19 symptoms with CXR imaging and optimize the X-ray imaging using segmentation thresholding algorithm-an evolutionary approach for bio-medical diagnosis. Int. J. Pharmacol., 18: 644-656.

Corresponding Author: N. Prabhakaran, Department of Biomedical Engineering, Agni College of Technology, Chennai, India

Competing Interest: The authors have declared that no competing interest exists.

Data Availability: All relevant data are within the paper and its supporting information files.

INTRODUCTION

The COVID-19 pandemic spreads quickly and infects a significant number of people around the world. The critical issue of COVID-19 symptoms being investigated by several researchers and scientists, with the aid of reducing virus spread. The critical task might include fever, cough, headache and diarrhea and also include pneumonia, respiratory infection and loss of blood affects the entire lungs system which is dangerous to all parts of the body. The developed and underdeveloped country testing of COVID-19 symptoms consists of 3 test they are Computed Tomography, RT-PCR test and Lung Ultrasound test. The Computed Tomography test analyzes 3-D radiographic image predicts the pixel through False Positive (FP), False Negative (FN), True Positive (TP) and True Negative (TN) with overlaying period. Similarly, Reverse Transcription-Polymerase Chain Reaction test requires an external kit to detect COVID-19 symptoms with the same period and prone to manual errors. Furthermore, the Lung Ultrasound Imaging system recognizes the symptoms of COVID-19 accurately when compared to another testing method. Despite Lung Ultrasound, Chest X-ray imaging requires less time to predict COVID-19 symptoms as early as possible. However, the cost of testing COVID-19 symptoms is less economical than the then previous existing method. The segmentation of Chest X-ray imaging predicts the earlier symptoms of COVID-19 and accurate analysis with predicted parameters. However, the radiographic technique also assists the visual features such as ground-glass opacities of detection of lung image based on cite score. The relevant features of Chest X-ray imaging predict automatic image segmentation and optimize the features of COVID-19. Furthermore, the Deep Learning technique segments image feature with the high-quality enhancement of Chest X-ray imaging observed by the radiologist with unknown error represents as True Negative in Chest X-ray imaging system. However, Chest X-ray imaging diagnoses the affected image not accurately as CNN Algorithm. The segmentation algorithm segments the Chest X-ray image of the COVID-19 patient predicts the accuracy of nearly 75% using Peripheral Ground Opacity (PGO). Initially, the radiographic technique enhances image features and assist in highlighting the medical center to collect and transport data at a certain distance. The Chest X-ray optimize the characteristic of COVID-19 and analyze the viral effect found in the Lung Ultrasound imaging system for procurement and maintenance. The proposed methodology of segmentation of COVID-19 analysis predicts the symptoms accurately concerning Ground Truth. Therefore, the predictive analysis of COVID-19 symptoms by Chest X-ray imaging verifies with ground truth and accuracy of delineation for feature enhancement and measurement. Detection of COVID-19 predicts the extraction of Chest X-ray imaging to determine image features by controlling the parameter of pneumonia, temperature and suffocation are the major problems in contour edge detection. In contour edge detection, the parameter recognized by the physician will take better decisions to reduce mortality rate when compared with the other existing method[1]. Furthermore, the segmentation algorithm will analyze the CXR image based on normal and abnormal detection of contour for feature extraction and measurement. Despite normal and abnormal contour detection, pleural changes are also occurring simultaneously in Chest X-ray imaging will accurately predict the symptoms of COVID-19[2]. Similarly, the RT-PCR kit samples the mucus fluid of COVID-19 symptoms which predicts positive or negative based on the test result recognized by the radiologist[3]. The radiologist with a lack of knowledge about COVID-19 symptoms facing a greater risk to detect normal and abnormal contour in Chest X-ray imaging. The contour extract feature for pixel size and shape and outer-performs the existing method which includes segmentation and classification of Chest X-ray imaging[4]. The Segmentation and classification of the labeled and unlabeled pixel with prior knowledge will diagnose the early detection of COVID-19 symptoms effectively[5]. The inhomogeneity in Chest X-ray imaging eliminates the error in pixel noise which is highly robust for contour edge detection with a specified region of interest (ROI)[6]. However, the detection of COVID-19 can also be tested by Computed Tomography (CT) image with a matrix method is employed for segmentation. The matrix method of Computed Tomography image verifies accurately for detection of virus in segmentation algorithm. The One-Dimensional segmentation matrix method implements with the flatted image for detection of contour and the Two-Dimensional segmentation matrix method occurs with a sliding window for detecting the changes inaccuracy. The One-Dimensional and Two-Dimensional matrix method compares with the existing method for predicting ground truth verify and highlights the symptoms[7]. The modeling analysis prevents the spreading of viruses from person to person highlights the phenomenal structure of virus in day-to-day life which saves human life age from 45-80 years as that of researcher identifies concerning the public database[8]. The number of datasets is available for public users to access and predict the feature extraction of Chest X-ray imaging analyze

automatically through the proposed segmentation algorithm. Similarly, the Deep Learning algorithm for the classification of segmented image accuracy will delineate feature extraction of Lung Ultrasound images[9]. The feature extraction of the pre-trained image with pixel classification of supervised and unsupervised images evaluates the performance of inhomogeneity and significantly predicts image abnormality such as size, shape and intensity with a non-contour edge detection algorithm[10]. Inhomogeneity in Chest X-ray image predicts the future enhancement method and justifies with false-negative pixel segmentation of Edge Detection Algorithm[11]. Despite the Edge detection method, the RT-PCR kit produces false negatives for clinical diagnosis with some delay in the initialization of treatment. The supervised Deep Learning method initializes the diagnosis process and segments the pixel with contour edge detection to maximize the integrity of solution space in the random variable of low energy function[12]. The Blue tooth low energy function of Too Close Too Long (TCTL) maintains a social distance of 6 feet and virus-free for prolonged life. The RSSI measurement and PACT measurement suggested evaluating Too Close for Too Long (TCTL) to maintain social distance even below 6 feet in solution space[13]. COVIDGR-1.0 maximizes the energy function by maintaining a different level of hierarchical structure for visual interpretation of Chest X-ray imaging[14]. Chest X-ray imaging optimizes the visual feature to gather a significant number of changes in a short time interval to prove accuracy. The accuracy predicted through the ACGAN model for future enhancement of imaging identifies with the visual model for surveying and reduce the spreading of the COVID-19 virus through proper channel[15]. The main theme of this study was the earlier prediction of viruses and reduces mortality rate. The enhancement of the segmentation thresholding algorithm accurately detected the prediction of COVID-19 symptoms with 90% of the enhanced image.

MATERIALS AND METHODS

Study area: Investigation and prediction of COVID-19 symptoms with CXR imaging are carried out in Royal Mother Hospital, K K Nagar, Chennai, India. The research was carried out from March, 2020 to April, 2021 for earlier prediction and diagnosis of COVID-19 symptoms. The investigation by radiologists brings accurate analysis and easier to malfunction with CXR imaging. The block diagram and performance of COVID-19 patients to analyze earlier detection was shown in Fig. 1. The datasets are available from a public database to segment and automatically classify the CXR image through various parameters results with Accuracy, Precision, F-measure and Recall. The proposed method of segmentation thresholding algorithm classifies for size, shape and intensity for feature enhancement and measurement through optimized image features. The image feature extracts the spreading of the virus in Chest X-ray image and investigates the performance of COVID-19 symptoms. The earlier prediction leads to reduce the mortality rate of the patient to live a healthy life. The accuracy of detection of COVID-19 symptoms proves with statistical parameters from Table 1-4. The accuracy of edge detection with and without contour proves from the statistical parameter. From statistical parameter symptoms of COVID-19 analysis and investigation by the radiologist proves with accuracy.

Enhancement of Chest X-ray image extract with a high feature through proposed segmentation algorithm indicates pixel intensity, non-homogeneity, etc. Fig. 2 represented the overall segmentation method for feature enhancement and prediction at a cross-section of (1×1) windowing technique where the input image (Fig. 2a) segment through energy function, according to the energy function histogram analysis of low frequency identifies with less noise as shown in

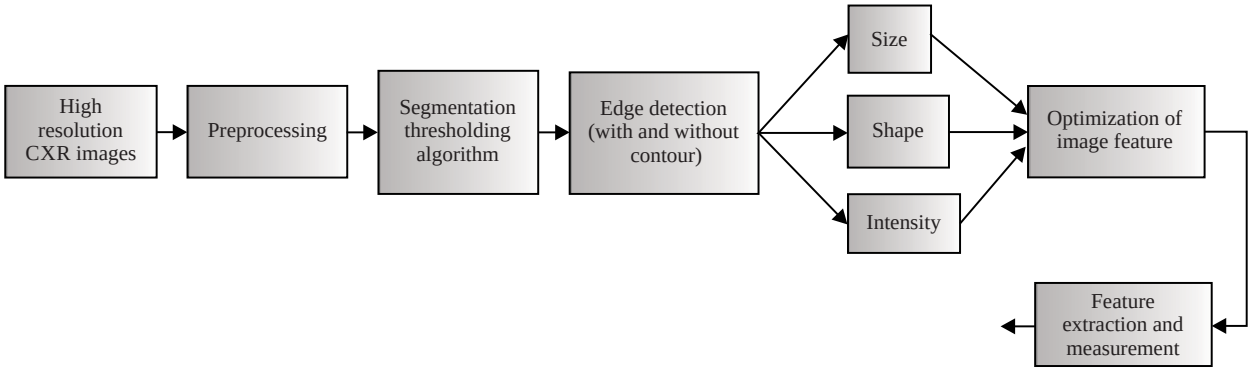

Fig. 1: Block diagram of predictive analysis of COVID-19 symptoms in the earlier stage

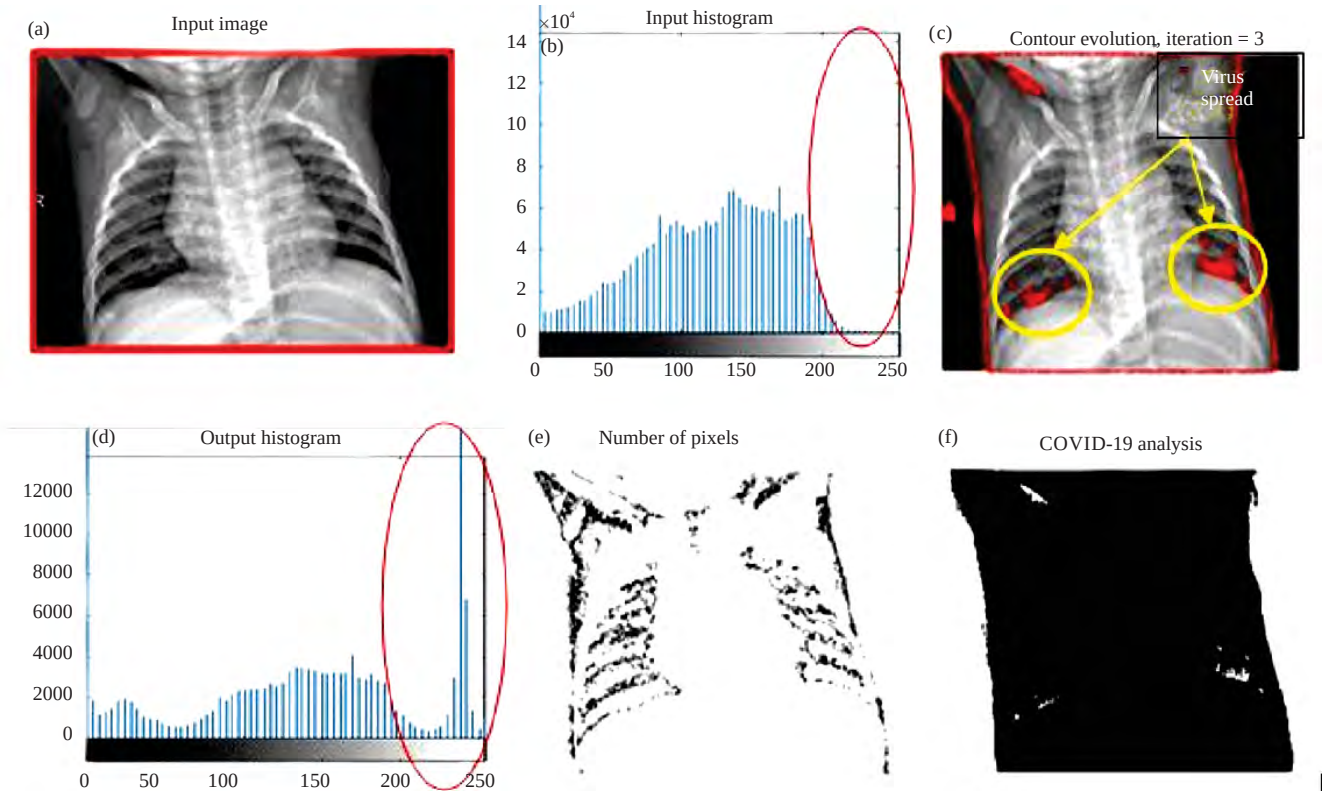

Fig. 2(a-f): Spreading of Infection through fever-chest X-ray Imaging, (a) input image, (b) histogram analysis of input, (c) contour detection, (d) histogram analysis of contour detection, (e) number of pixels through segmentation thresholding algorithm, (f) ground truth verification of COVID-19 - parameter fever analysis

Table 1: Statistical parameter for extraction of fever

	Input detection		Contour edge detection 1		Contour edge detection 2		Contour edge detection 3	
Parameters	With contour	Without contour	With contour	Without contour	With contour	Without contour	With contour	Without contour
Accuracy	0.614	0.602	0.701	0.682	0.741	0.722	0.781	0.612
Precision	0.602	0.591	0.621	0.601	0.682	0.645	0.615	0.608
F-Measure	0.599	0.543	0.636	0.598	0.676	0.634	0.648	0.591
Recall	0.532	0.506	0.589	0.545	0.624	0.604	0.518	0.502

Table 2: Statistical parameter for extraction of pneumonia

	Input detection		Contour edge detection 1		Contour edge detection 2		Contour edge detection 3	
Parameters	With contour	Without contour	With contour	Without contour	With contour	Without contour	With contour	Without contour
Accuracy	0.618	0.594	0.648	0.645	0.658	0.649	0.648	0.684
Precision	0.681	0.595	0.615	0.662	0.649	0.686	0.654	0.648
F-Measure	0.691	0.535	0.672	0.618	0.654	0.618	0.617	0.615
Recall	0.657	0.618	0.648	0.648	0.648	0.656	0.605	0.604

Table 3: Statistical parameter for extraction of mucus fluid

	Input detection		Contour edge detection 1		Contour edge detection 2		Contour edge detection 3	
Parameters	With contour	Without contour	With contour	Without contour	With contour	Without contour	With contour	Without contour
Accuracy	0.618	0.622	0.641	0.675	0.647	0.674	0.698	0.678
Precision	0.645	0.685	0.695	0.645	0.632	0.675	0.642	0.687
F-Measure	0.648	0.635	0.674	0.699	0.641	0.632	0.645	0.685
Recall	0.628	0.647	0.696	0.644	0.674	0.610	0.646	0.695

Table 4: Statistical parameter for extraction of respiratory system

	Input detection		Contour edge detection 1		Contour edge detection 2		Contour edge detection 3	
Parameters	With contour	Without contour	With contour	Without contour	With contour	Without contour	With contour	Without contour
Accuracy	0.611	0.654	0.684	0.649	0.549	0.613	0.518	0.679
Precision	0.615	0.625	0.585	0.532	0.548	0.546	0.618	0.619
F-Measure	0.647	0.664	0.617	0.545	0.618	0.617	0.628	0.589
Recall	0.682	0.624	0.618	0.694	0.571	0.647	0.549	0.518

Fig. 2b. In Fig. 2c, the output image compares with the input image at the high-frequency range, the red color portion highlights the effect of the virus in the lungs. Histogram analysis of input compares with output histogram the prediction of virus spread indicates in low-frequency range as shown in Fig. 2d. The threshold level of segmentation delineates the spreading of the virus in the human lung accurately predicted and justify in Fig. 2e, described the pixel-level segmentation of classes. The segmentation of processed image with minimum iteration value and analysis of COVID-19 with True positive and False positive pixel represents in Fig. 2f, which indicated in a black mask to delineate the accuracy. The statistical characteristics of virus prediction with and without contour accuracy of about 69% from the cite score was shown in Table 1. The image enhancement of energy function with and without contour was represented in Eq. 1-6:

$$E_{ROI} = E_{ob}(\emptyset) + E_{ib}(\emptyset) \quad (1)$$

Where:

E_{ROI} = Energy concerning region of interest
E_{ob} = Energy concerning outer boundary
E_{ib} = Energy concerning inner boundary

The outer boundary energy function E_{ob} is determined by region, gradient and No. of pixels, while the inner boundary energy function E_{ib} is used as a constraint for the evolution of the level-set. From Fig. 2, images with intensity, non-homogeneity, the pixels are clustered and the pixels with similar intensity and pixel intensity values are assigned to both Ωib and Ωob. Thus, the proposed outer boundary energy function E_{ob} proposes the pixel information intensity for both Ωib and Ωob of the given input image:

$$E_{ob} = \propto\left[\int_{\Omega} hY_{ib}(x) H_{\varepsilon}(\emptyset)\,dx + \int_{\Omega} hY_{ob}(x)\left(1 - H_{\varepsilon}(\emptyset)\right)dx\right] + \lambda\left[\int_{\Omega} hZ_{in}(x) H_{\varepsilon}(\emptyset)\,dx + \int_{\Omega} hZ_{ob}(x)\left(1 - H_{\varepsilon}(\emptyset)\right)dx\right] \quad (2)$$

Where:

$$Y_{ib}(x) = [S(x) - s_1]^2 \quad (3)$$

$$Y_{ob}(x) = [S(x) - s_2]^2 \quad (4)$$

$$Z_{ib} = |I(x) - c_1|^2 + |I(x) - f|^2 \quad (5)$$

$$Z_{ob} = |I(x) - c_2|^2 \quad (6)$$

Extraction of segmented Chest X-ray Image spread within 3 days and affect the lung by nearly 25% of the output image. The accuracy is detected by the segmentation algorithm delineate the edge detection with and without contour for ground truth verification in the earlier stage of virus spread.

The initial stage of virus infection of Chest X-ray image of 3 days when compared with the input of Chest X-ray image with contour edge detection 1 the output image is enhanced by 11.41% of the input image as shown in Table 3. Contour Edge Detection 2 the output image is enhanced by 13.06% of the input image. At last contour Edge Detection 3, the output image is enhanced by 14.71% of the input image.

And then without contour edge detection 1, the output image is enhanced by 11.32% of the input image. And contour Edge Detection 2 the output image is enhanced by 12.99% of the input image. At last contour Edge Detection 3, the output image is enhanced by 14.16% of the input image.

The overall spreading of the virus through the segmentation algorithm was shown in Fig. 3. The input image Fig. 3a processed with the segmentation algorithm where the accuracy is null deflection. The input image Fig. 3a compared with histogram analysis of the image Fig. 3b the higher frequency part the noise is less when compared to Fig. 2. However, the image is slid with a cross-section of (3×3) windowing technique with maximum iteration the spreading of the virus increases when compared to the input image Fig. 3a and the output is represented in Fig. 3c. The histogram analysis of input compares with histogram analysis of output error is accurately predicted as shown in Fig. 3d whereas the accuracy is proved in the higher frequency range. In Fig. 3e, the threshold level of segmentation accurately predicts the spread of the virus in the human lung by segmentation method. Figure 3f, shows segmentation with the smallest iteration value and COVID-19 analysis of True Positive and False Positive pixels are masked in black color and accuracy is delineated. The Feature Extraction of Chest X-ray image with

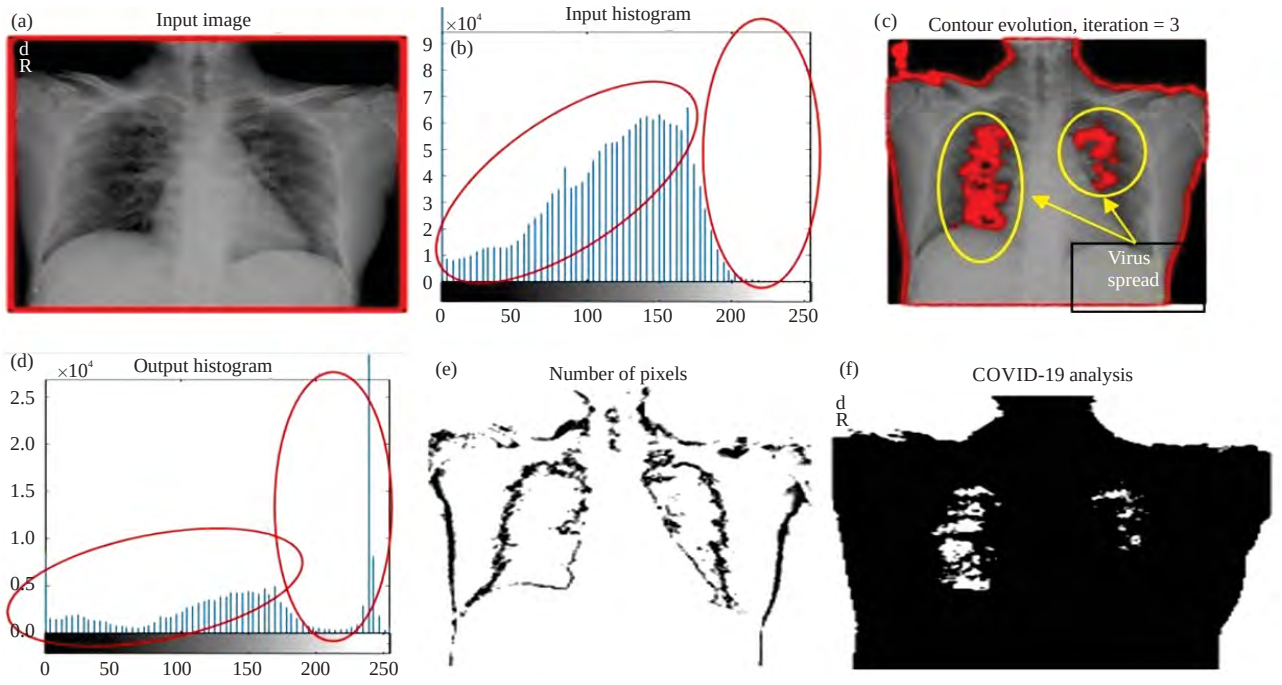

Fig. 3(a-f): Spreading of infection through pneumonia-chest X-ray imaging, (a) input image (b) histogram analysis of input (c) contour detection (d) histogram analysis of contour detection (e) number of pixels through segmentation thresholding algorithm, (f) ground truth verification of COVID-19 - parameter pneumonia analysis

and without contour edge detection were represented in the equation From 7-11.

ε is the Heaviside function and scaling constants for pixel information. In addition, both pixel information and energy functions are embedded with a boundary edge detector, h, described as:

$$h = \frac{1}{1+\left|\nabla_{kp} * I\right|^2} \tag{7}$$

where, r and k_p are the gradient operator and Gaussian kernel with standard deviation ρ. In addition, * is the convolution operator that reduces the influence of intense noise:

$$S(x) = |\bar{I}(x) - I_k(x)|^2 \tag{8}$$

where, I the means pixel value of I and $I_k = k_\rho * I$ is the image blurred by the Gaussian filter. Moreover, s_1 and s_2 are the saliency means for Ωin and Ωop:

$$s_1 = \frac{\int_\Omega S(x).H_\varepsilon(\varnothing)\,dx}{\int_\Omega H_\varepsilon(\varnothing)\,dx} \tag{9}$$

$$s_2 = \frac{\int_\Omega S(x).(1-H_\varepsilon(\varnothing))\,dx}{\int_\Omega (1-H_\varepsilon(\varnothing))\,dx} \tag{10}$$

$$\begin{aligned} c_1 &= \omega.\text{mean}\left(I(x)\,\varepsilon\Omega_{in}\right) \\ c_2 &= \omega.\text{mean}\left(I(x)\,\varepsilon\Omega_{op}\right) \\ f &= \omega.\text{median}\left(I(x)\,\varepsilon\Omega_{in}\right) \end{aligned} \tag{11}$$

The stage of virus infection of the Chest X-ray image of 11 days when compared with the input of the Chest X-ray image with contour edge detection 1 the output image is enhanced by 11.41% of the input image (Table 2). And contour Edge Detection 2 the output image is enhanced by 13.06% of the input image. At last contour Edge Detection 3, the output image is enhanced by 14.71% of the input image. And then without contour edge detection 1, the output image is enhanced by 11.32% of the input image. And contour Edge Detection 2 the output image is enhanced by 12.99% of the input image. At last contour Edge Detection 3, the output image is enhanced by 14.16% of the input image.

Figure 4 showed the prediction of virus spread from the input image Fig. 4a at a crosswise of (5×5) windowing technique wherever the input image (a) segment through energy function, in step with the energy operate input histogram analysis of low frequency identifies with less noise as shown in Fig. 4b. In Fig. 4c, the output image compares with the input image at high frequency vary, the red color portion highlights the result as virus spread in lungs. Histogram analysis of input compares with output histogram

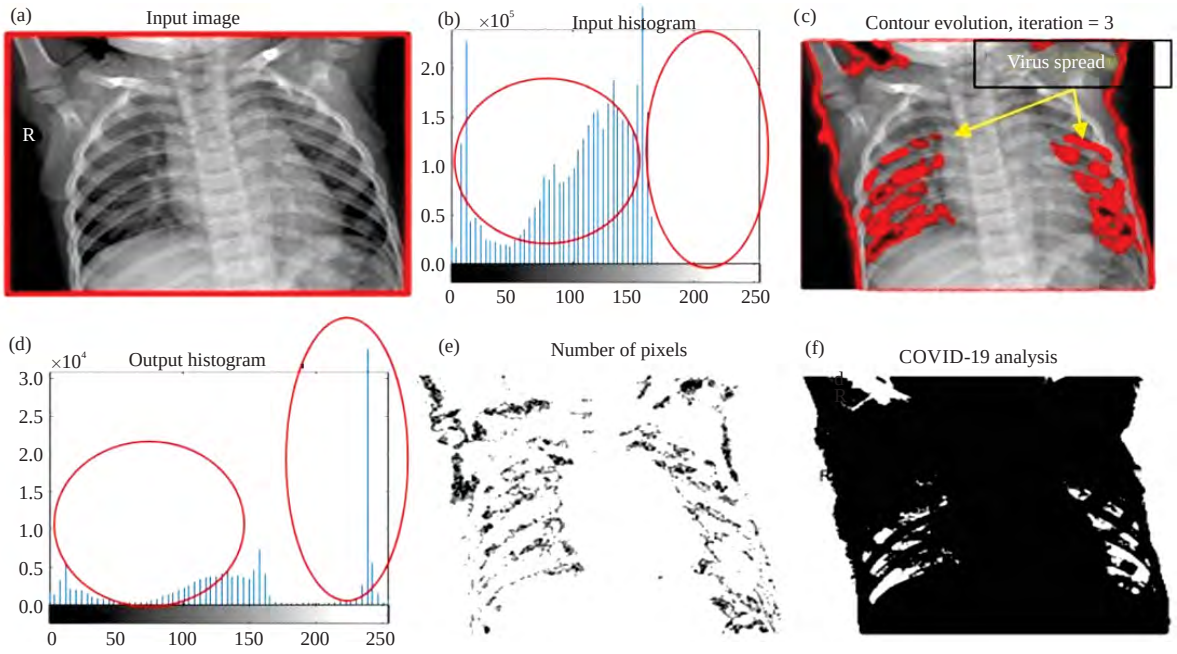

Fig. 4(a-f): Spreading of infection through mucus fluid-chest X-ray imaging, (a) input image (b) histogram analysis of input (c) contour detection (d) histogram analysis of contour detection (e) number of pixels through segmentation thresholding algorithm. (f) ground truth verification of COVID-19 - parameter mucus fluid analysis

the prediction of virus unfold indicates in low frequency vary as shown in Fig. 4d. The level of segmentation delineates the spreading of the virus within the human respiratory organ accurately expected and justifies in Fig. 4e describes the picture element level segmentation of categories. The segmentation was processed with minimum iteration value and analysis of COVID-19 of True positive and False positive imaging represented in Fig. 4f that use a black mask to outline the accuracy. Table 3 showed the applied characteristics of virus prediction with and without contour detection accuracy of 89% from the citing score. The Image enhancement of the Energy function operates with and without contour delineate in equation from 12-15:

$$\omega = \int_{\Omega} H_{\varepsilon}(\varnothing)\left\|Z_{in}\right\|_2 dx + \int_{\Omega}\left(1 - H_{\varepsilon}(\varnothing)\right)\left\|Z_{op}\right\|_2 dx \quad (12)$$

where, ||.|| is the L2 norm. Compared to the mean values, the median is closer to the pixel value of the image boundary, which can effectively suppress the noise and retain more detailed features such as thin lines.

However, only with the output energy function, the segmentation may be inaccurate and irregular and some singularities or undesired false contours may appear. Therefore, the input energy function is given for approval:

$$E_{ib}(\varnothing) = \frac{\mu L(\varnothing)\eta(I)}{Max\left(\left|\eta(I)\right|\right)} + \nu P(\varnothing) \quad (13)$$

where, μ, ν>0 are constants. Terms l (Ø) and P (Ø) are the weighted length term of the contour dealing with an object's boundary based on edge information:

$$l(\varnothing) = \int_{\Omega} h\delta_{\varepsilon}(\varnothing)\left|\nabla_{\varnothing}\right| dx \quad (14)$$

$$P(\varnothing) = \int_{\Omega} \frac{1}{2}\left(1 - \left|\nabla_{\varnothing}\right|\right)^2 dx \quad (15)$$

where, E_{ib} is to regularize Ø with the use of P (Ø) such that the contour remains close to the ROC and prevents the appearance of singularity for smooth contour evolution.

Table 3 manifested the initial stage of virus infection of the Chest X-ray image of 3 days when compared with the input of the Chest X-ray image with contour edge detection 1 the output image is enhanced by 11.37% of the input image. And contour Edge Detection 2 the output image is enhanced by 14.79% of the input image. At last contour Edge Detection 3, the output image is enhanced by 15.46% of the input image. And then without contour edge detection 1, the

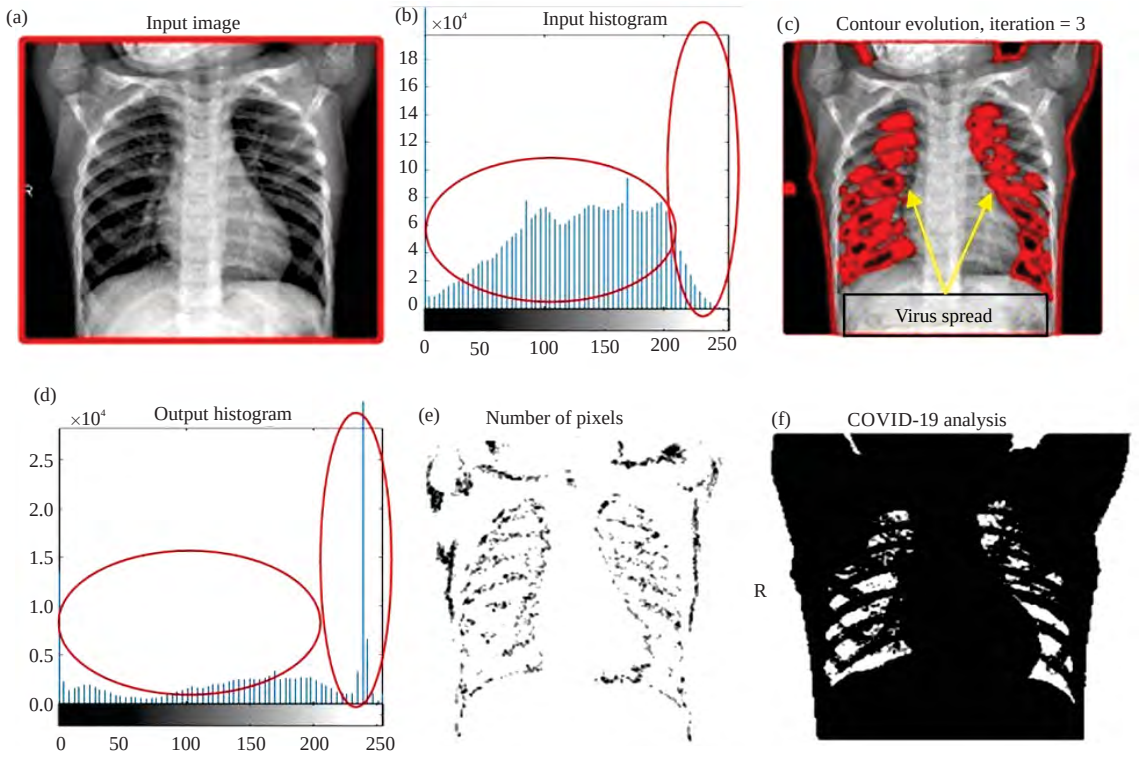

Fig. 5(a-f): Spreading of infection through respiratory system-chest X-ray imaging, (a) input image (b) histogram analysis of input (c) contour detection (d) histogram analysis of contour detection (e) number of pixels through segmentation thresholding algorithm. (f) ground truth verification of COVID-19 - parameter respiratory system analysis

output image is enhanced by 10.85% of the input image. And contour Edge Detection 2 the output image is enhanced by 12.83% of the input image. At last contour Edge Detection 3, the output image is enhanced by 14.90% of the input image.

In Fig. 5, the spreading of virus through the segmentation algorithm method the input image Fig. 5a processed with the segmentation algorithm technique the accuracy is null deflection. The input image Fig. 5a compares with histogram analysis of the image Fig. 5b for the prediction of virus spread level in human lungs. However, the image is slid with a cross-sectional of (7×7) windowing technique with several iterations the spreading of the virus will increase in comparison to the input image Fig. 5a and also the output is delineated in Fig. 5c. The histogram analysis of input compares with histogram analysis of output error is accurately delineated as high frequency is shown in Fig. 5d. In Fig. 5e, the edge level of segmentation accurately predicts the spreading level of the virus within the human respiratory organ by the segmentation method. Figure 5f shows segmentation with iteration and COVID-19 analysis of True Positive and False Positive pixels which delineate the accuracy with a black mask. Table 4 represented the applied characteristics of virus prediction with and without contour detection at the rate of 92% from the citing score. The Feature Extraction of Chest X-ray image with and without contour edge detection measured using the Eq.16-22:

$$\eta\,(I) = \mathrm{sgn}\,(2c_1+2f-4c_2).\ \mathrm{sgn}\,(\gamma).\ \gamma^2 \tag{16}$$

Where:

$$\gamma = I\,(x) - \frac{c_1^2 + f^2 - 2c_2^2}{2c_1 + 2f - 4c_2} \tag{17}$$

In Fig. 5, the development of COVID-19 in Chest X-ray Image is at the stage of 19 days. The chest X-ray image is segmented to predict COVID-19 spreadability from the given input image. The input histogram is classified with output histogram for the accurate prediction of COVID-19 virus spread in the Chest X-ray image. Comparably, the highest frequency part of the noise is suppressed and extraction of COVID-19 with an accuracy of detection of the virus is fine-tuned. Segmentation of Chest X-ray image extract with the necessary information of virus spread throughout the lungs.

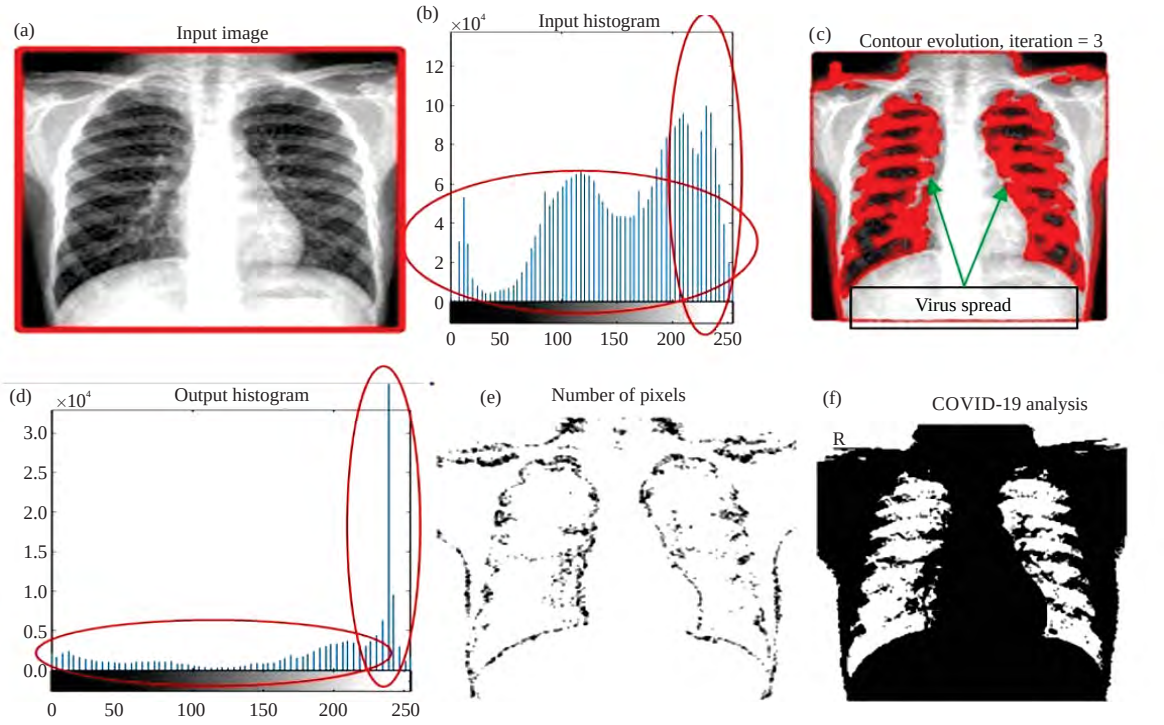

Fig. 6(a-f): Comparison of infection rate of fever, pneumonia, mucus fluid, respiratory system-chest X-ray imaging, (a) input image (b) histogram analysis of input (c) contour detection (d) histogram analysis of contour detection (e) number of pixels through segmentation thresholding algorithm. (f) ground truth verification and comparison analysis of fever, pneumonia, mucus fluid and respiratory system COVID-19 - parameter analysis

The affection of the virus is very harmful and it should be detected in the earlier stage of COVID-19 analysis of the segmentation algorithm.

The initial stage of virus infection of Chest X-ray image at the stage of 19 days was exhibited in Table 4. The input of Chest X-ray image with contour edge detection 1 the output image is enhanced by 12.19% of the input image. And contour Edge Detection 2 the output image is enhanced by 13.85% of the input image. At last contour Edge Detection 3, the output image is enhanced by 15.77% of the input image. And then without contour edge detection 1, the output image is enhanced by 11.23% of the input image. And contour Edge Detection 2 the output image is enhanced by 12.73% of the input image. At last contour Edge Detection 3, the output image is enhanced by 14.82% of the input image.

The proposed energy function E_{ROI} can be rewritten as:

$$\begin{aligned} E_{ROI}(\varnothing) = \propto & \left[\int_{\Omega} hY_{ib}(x)H_{\varepsilon}(\varnothing)dx + \int_{\Omega} hY_{ob}(x)\left(1-H_{\varepsilon}(\varnothing)\right)dx\right] \\ & + \lambda\left[\int_{\Omega} hZ_{ib}(x)H_{\varepsilon}(\varnothing)dx + \int_{\Omega} hZ_{ob}(x)\left(1-H_{\varepsilon}(\varnothing)\right)dx\right] \\ & + \frac{\mu\eta(I)}{Max\left(|\eta(I)|\right)}\int_{\Omega} h\delta_{\varepsilon}(\varnothing)|\nabla_{\varnothing}|dx + \frac{\nu}{2}\int_{\Omega}\left(1-|\nabla_{\varnothing}|\right)^2 dx \end{aligned} \quad (18)$$

Further, ∂ to minimize to Ø, the derivative can be written by the calculus of variations:

$$\begin{aligned} \frac{\partial E_{ROI}}{\partial\varnothing} = & \alpha\left[h\left(S(x)-s_1\right)^2 - h\left(S(x)-s_2\right)^2\right] \\ & + \lambda\left[h\left(\left|I(x)-c_1\right|^2 + \left|I(x)-f\right|^2\right) - \left|I(x)-c_2\right|^2\right] \\ & - \frac{\mu L(\varnothing)\eta(I)}{Max\left(|\eta(I)|\right)}\delta_{\varepsilon}(\varnothing)\,div\left(h\frac{\nabla_{\varnothing}}{|\nabla_{\varnothing}|}\right) - \nu\Delta\varnothing \end{aligned} \quad (19)$$

$$\begin{aligned} \frac{\partial\varnothing}{\partial t} = -\frac{\partial E_{ROI}}{\partial\varnothing} = & -\alpha h\left[Y_{ib}(x)-Y_{ob}(x)\right] - \lambda h\left[Z_{ib}(x)-Z_{ob}(x)\right] \\ & + \frac{\mu L(\varnothing)\eta(I)}{Max\left(|\eta(I)|\right)}\delta_{\varepsilon}(\varnothing)\,div\left(h\frac{\nabla_{\varnothing}}{|\nabla_{\varnothing}|}\right) + \nu\Delta\varnothing \end{aligned} \quad (20)$$

Figure 6 represented the prediction of virus spread at a cross-section of (9×9) windowing technique from the input image Fig. 6a through energy function from the above-mentioned equations. Input histogram analysis of low frequency identifies with less noise as shown in Fig. 6b. In Fig. 6c, the output image compares with the input image at high frequency, the red color portion highlights the final result as the virus spreads in the lungs. Histogram analysis of input

Table 5: Statistical parameter for extraction of fever, pneumonia and COVID-19

	Input detection		Contour edge detection 1		Contour edge detection 2		Contour edge detection 3	
Parameters	With contour	Without contour	With contour	Without contour	With contour	Without contour	With contour	Without contour
Accuracy	0.648	0.655	0.676	0.574	0.548	0.502	0.674	0.517
Precision	0.594	0.608	0.545	0.657	0.674	0.645	0.657	0.563
F-Measure	0.655	0.685	0.685	0.648	0.536	0.578	0.696	0.596
Recall	0.568	0.597	0.554	0.585	0.687	0.536	0.563	0.674

compares with output histogram the prediction of virus unfold indicates in low frequency vary as shown in Fig. 6d. The segmentation algorithm delineates the spreading of the virus in evolution iteration the human lungs accurately justified. Figure 6e describes the image component level segmentation of classes. The segmentation processed with minimum iteration price and analysis of COVID-19 of True positive and False positive imaging portrayed in Fig. 6f, which use a black mask to delimit the accuracy. The applied characteristics of virus prediction with and while not contour detection accuracy of a toilet from citing score was shown in Table 3. The Image sweetening of Energy perform operate with and while not contour delineates in Eq. 12-15.

In the proposed Region of Interest model, the region information is a global feature determined by I. Therefore, the initialization Ø can be very flexible. The proposed ROI's level-set function is initialized as:

$$\emptyset_{t=0} = p,\ x \in \Omega \tag{21}$$

$$\left|\frac{\partial \emptyset}{\partial t}\Delta t\right| = \left|\emptyset_{t+1} - \emptyset_{t}\right| < \gamma \tag{22}$$

The initial stage of virus infection of Chest X-ray image at the final stage of 21 days was conveyed in Table 5. The output image when compared with the input of Chest X-ray image with contour edge detection 1 the output image is enhanced by 12.32% of the input image. And contour Edge Detection 2 the output image is enhanced by 14.56% of the input image. At last contour Edge Detection 3, the output image is enhanced by 16.01% of the input image. And then without contour edge detection 1, the output image is enhanced by 11.63% of the input image. And contour Edge Detection 2 the output image is enhanced by 12.66% of the input image. At last contour Edge Detection 3, the output image is enhanced by 14.93% of the input image.

RESULTS

The Relationship between symptoms of COVID-19 with and without contour detection was shown in Fig. 7. The curve differentiates the difference between fever, pneumonia and COVID-19 are plotted to delineate the accuracy (Fig. 7a). The characteristics of fever accuracy of about 50% are detected from dataset 1, pneumonia accuracy of 52.5% is detected and COVID-19 detects about 68% which proves that initial stage of symptoms. In Fig. 7b detection of accuracy concerning fever 54%, pneumonia 60% and COVID-19 68% is detected. In Fig. 7c, changes of accuracy in fever 62%, pneumonia 74% and COVID-19 76% prove with accuracy with statistical table represented from Table 1-5. In Fig. 7d, spreads symptoms of COVID19 fever 63.5%, pneumonia 64% and COVID-19 70%. The high mortality symptoms indicate in Fig. 7e represent the percentage of fever 70, pneumonia 78% and COVID-19 92% which spread the entire parts of the lungs. The proposed method of segmentation algorithm delineates the ground truth verification with the accuracy of all the datasets through the threshold method of detection 82% of the affected images.

DISCUSSION

Earlier prediction of COVID-19 symptoms by the Too Close Too Short technique spreads virus from person to person within 3-21 days. However, if the virus spread increases from 3-21 working days, a huge increase in the mortality rate is predicted by the Indian Council of Medical Research (ICMR). The virus spread to be stopped immediately by analyzing the concept of too close too short and reduce the mortality rate by the proposed segmentation thresholding algorithm. The proposed segmentation thresholding algorithm finds the spread within 3 hrs once the person is infected from the virus and accuracy is predicted through the statistical parameter from the Table 1-4. The previous method use machine learning, fuzzy c-means clustering algorithm and Adaptive neural network finds the symptoms of COVID-19 prediction is very difficult to analyze within 3-21 days. Nowadays without any symptoms, the spread increases rapidly, while testing it confirms that the COVID-19 is positive. The proposed method also highlights with or without the symptoms of COVID-19, earlier prediction is analyzed within 3-21 days of corona affected person. Different parameters are analyzed in our

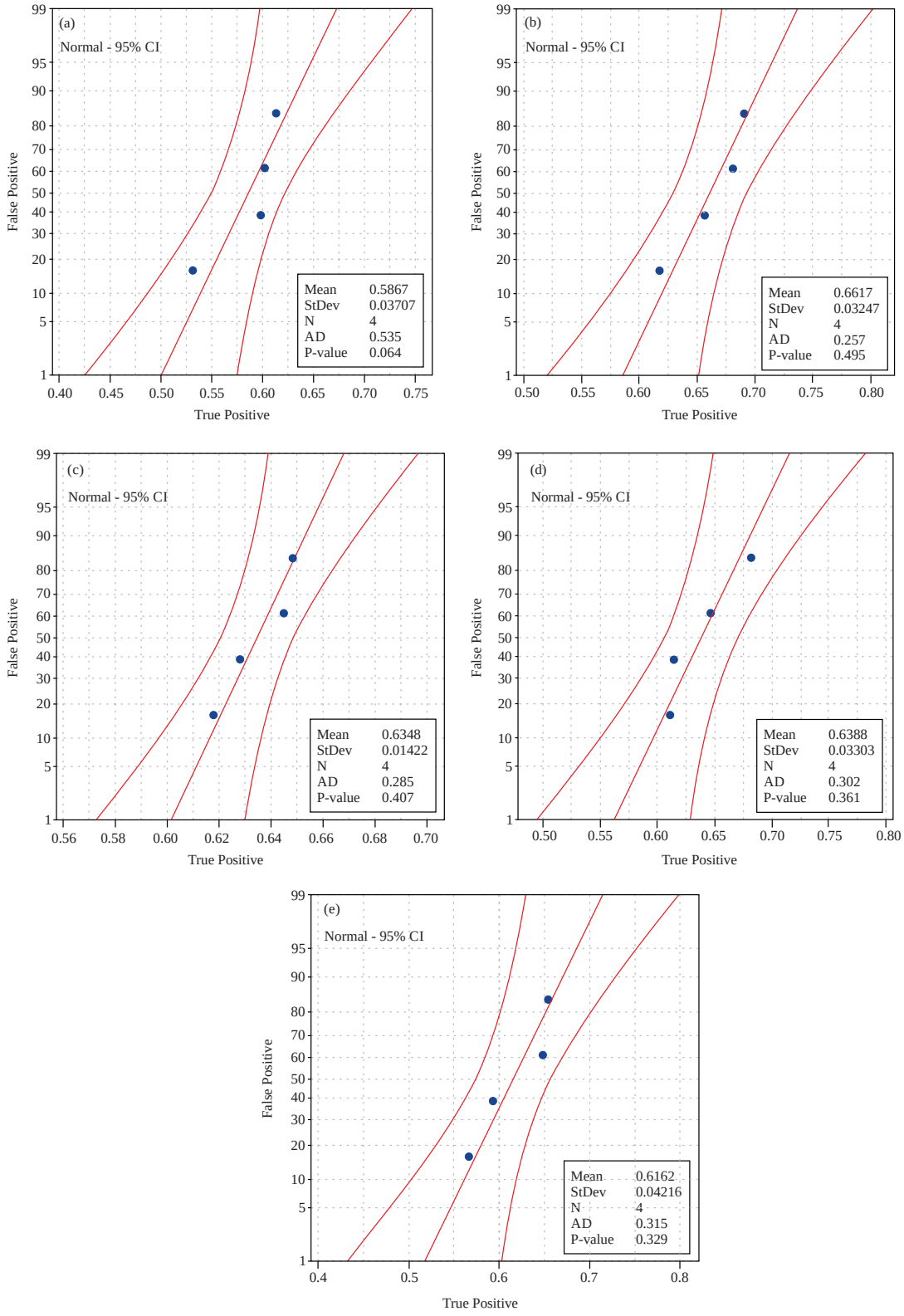

Fig. 7(a-e): Relationship curve with the maturity period of 3-21 days of COVID-19 symptoms, (a) parameter analysis of fever (b) parameter analysis of pneumonia (c) parameter analysis of mucus fluid (d) parameter analysis of respiratory systems (e) comparison of fever, pneumonia, mucus fluid and respiratory system

study such as fever, pneumonia, mucus fluid and respiratory system are the causes of prediction of COVID-19. When compared with the previous method the error analyzed by different optimization algorithms and segmentation algorithms is not predicted well in advance. Furthermore, the parameter predicts the symptoms of COVID-19 for future enhancement and measurement.

In 2020, automatic detection of COVID-19 analysis is analyzed and segmented through RX image with a parameter such as control and pneumonia results in providing evidence to analyze symptoms of COVID-19 with two parameters. However, the prediction and classification are not accurate. In a conclusion, the author's study into the parameters of fever, pneumonia, mucus fluid and respiratory system proves with high accuracy from 3-21 working days.

In 2020, COVID-19 analysis based on ROI with existence with noise and in homogeneity in pixel intensity. The performance is evaluated on complex, real and synthetic images to analyze the symptoms of COVID-19 which take huge processing time in the state of art. However, the processing time is ultimately reduced in the proposed finding which highlights the future enhancement and measurement in the earlier stage.

In 2020, detection of COVID-19 symptoms by Spatio-Temporal dataset is pre-processed by neighborhood pixels to reduce the error in multivariate and by training the dataset the COVID-19 symptoms are predicted. However, without a multivariate dataset, the image is segmented through state of art and prediction of symptoms highlights the features.

The radiologist uses the dataset COVIDGR-1.0 for segmentation, data augmentation and transformation of data to predict the earlier symptoms with a CXR image for better performance. Without magnifying, the augmentation process prediction proves and highlights feature enhancement.

ACGAN generates and predicts the symptoms of COVID-19 by enlarging the high-resolution image with a huge amount of datasets for the researcher in the medical sector. The radiologist without enlarging the resolution of the image feels comfortable and predicts the symptoms of COVID-19 with a fewer number of datasets.

Performance evaluation using Bluetooth LE signal with a concept of Too Close Too Long indicates the social distance to reduce virus spread from proximity effect. This method elucidates for prediction but the proposed method without proximity effect the symptoms are predicted and diagnosed in an earlier stage (2021).

In 2021, images were analyzed with the conditional generative adversarial network through CT images with two parameters i.e., ground-glass opacity and consolidation. The method analyzed synthesize the state of art and proved to be a cost-effective technique. Similarly, the proposed finding is low cost effective.

CONCLUSION

Segmentation of Chest X-ray images enhanced for feature extraction and measurement accurately predict the mortality rate. The spreading of the virus is rapidly increasing and diagnose the symptoms of COVID-19 is very critical. The proposed segmentation method verifies the ground truth verification accurately the symptoms of COVID-19 even uncritically.

SIGNIFICANCE STATEMENT

COVID-19 symptom analysis predicted in the earlier stage to reduce the mortality rate. The parameters of fever, pneumonia, mucus fluid and respiratory system are predicted in the earlier stage, once predicted diagnosed automatically through segmentation thresholding algorithm. The accuracy of detection of symptoms proves with ground truth verification.

REFERENCES

1. Arias-Londono, J.D., J.A. Gomez-Garcia, L. Moro-Velazquez and J.I. Godino-Llorente, 2020. Artificial intelligence applied to chest X-ray images for the automatic detection of COVID-19. A thoughtful evaluation approach. IEEE Access, 8: 226811-226827.
2. Dong, D., Z. Tang, S. Wang, H. Hui and L. Gong *et al*., 2021. The role of imaging in the detection and management of COVID-19: A review. IEEE Rev. Biomed. Eng., 14: 16-29.
3. Gharizadeh, B., J. Yue, M. Yu, Y. Liu, M. Zhou, D. Lu and J. Zhang, 2021. Navigating the pandemic response life cycle: Molecular diagnostics and immunoassays in the context of COVID-19 management. IEEE Rev. Biomed. Eng., 14: 30-47.
4. Jiang, Y., H. Chen, M. Loew and H. Ko, 2021. COVID-19 CT image synthesis with a conditional generative adversarial network. IEEE J. Biomed. Health Inf., 25: 441-452.
5. Joshi, A., M.S. Khan, S. Soomro, A. Niaz, B.S. Han and K.N. Choi, 2020. SRIS: Saliency-based region detection and image segmentation of COVID-19 infected cases. IEEE Access, 8: 190487-190503.
6. Karadayi, Y., M.N. Aydin and A.S. Ogrenci, 2020. Unsupervised anomaly detection in multivariate spatio-temporal data using deep learning: Early detection of COVID-19 outbreak in Italy. IEEE Access, 8: 164155-164177.

7. Liu, Q., C.K. Leung and P. Hu, 2020. A two-dimensional sparse matrix profile densenet for COVID-19 diagnosis using chest CT images. IEEE Access, 8: 213718-213728.
8. Marmarelis, V.Z., 2020. Predictive modeling of COVID-19 data in the us: Adaptive phase-space approach. IEEE Open J. Eng. Med. Biol., 1: 207-213.
9. Peng, Y., Y. Tang, S. Lee, Y. Zhu, R.M. Summers and Z. Lu, 2021. COVID-19-CT-CXR: A freely accessible and weakly labeled chest X-ray and CT image collection on COVID-19 from biomedical literature. IEEE Trans. Big Data, 7: 3-12.
10. Rajaraman, S., J. Siegelman, P.O. Alderson, L.S. Folio, L.R. Folio and S.K. Antani, 2020. Iteratively pruned deep learning ensembles for COVID-19 detection in chest X-rays. IEEE Access, 8: 115041-115050.
11. Sakib, S., T. Tazrin, M.M. Fouda, Z.M. Fadlullah and M. Guizani, 2020. DL-CRC: Deep learning-based chest radiograph classification for COVID-19 detection: A novel approach. IEEE Access, 8: 171575-171589.
12. Shi, J., X. Yuan, M. Elhoseny and X. Yuan, 2020. Weakly supervised deep learning for objects detection from images. Stud. Distributed Intell., 8: 231-242.
13. Su, Z., K. Pahlavan and E. Agu, 2021. Performance evaluation of COVID-19 proximity detection using bluetooth LE signal. IEEE Access, 9: 38891-38906.
14. Tabik, S., A. Gomez-Rios, J.L. Martin-Rodriguez, I. Sevillano-Garcia and M. Rey-Area *et al*., 2020. COVIDGR dataset and COVID-SDNet methodology for predicting COVID-19 based on chest X-ray images. IEEE J. Biomed. Health Inf., 24: 3595-3605.
15. Waheed, A., M. Goyal, D. Gupta, A. Khanna, F. Al-Turjman and P.R. Pinheiro, 2020. CovidGAN: Data augmentation using auxiliary classifier GAN for improved COVID-19 detection. IEEE Access, 8: 91916-91923.